Published in final edited form as:
Cancer Res. 2014 February 15; 74(4): 1250–1260. doi:10.1158/0008-5472.CAN-13-1778.

Curcumin targets breast cancer stem-like cells with microtentacles that persist in mammospheres and promote reattachment

Monica S. Charpentier[1,2], **Rebecca A. Whipple**[1], **Michele I. Vitolo**[1,3], **Amanda E. Boggs**[1,2], **Jana Slovic**[1,2], **Keyata N. Thompson**[1], **Lekhana Bhandary**[1,2], and **Stuart S. Martin**[1,2,3]

[1]Marlene and Stewart Greenebaum National Cancer Institute Cancer Center, University of Maryland School of Medicine, Baltimore, Maryland [2]Program in Molecular Medicine, University of Maryland School of Medicine, Baltimore, Maryland. [3]Department of Physiology, University of Maryland School of Medicine, Baltimore, Maryland.

Abstract

Cancer stem-like cells (CSC) and circulating tumor cells (CTCs) have related properties associated with distant metastasis, but the mechanisms through which CSCs promote metastasis are unclear. In this study, we report that breast cancer cell lines with more stem-like properties display higher levels of microtentacles (McTNs), a type of tubulin-based protrusion of the plasma cell membrane which forms on detached or suspended cells and aid in cell reattachment. We hypothesized that CSCs with large numbers of McTNs would more efficiently attach to distant tissues, promoting metastatic efficiency. The naturally occurring stem-like subpopulation of the HMLE breast cell line presents increased McTNs compared to its isogenic non-stem-like subpopulation. This increase was supported by elevated α-tubulin detyrosination and vimentin protein levels and organization. Increased McTNs in stem-like HMLEs promoted a faster initial reattachment of suspended cells that was inhibited by the tubulin-directed drug, colchicine, confirming a functional role for McTN in stem cell reattachment. Moreover, live cell confocal microscopy showed that McTN persist in breast stem cell mammospheres as flexible, motile protrusions on the surface of the mammosphere. While exposed to the environment, they also function as extensions between adjacent cells along cell-cell junctions. We found that treatment with the breast CSC-targeting compound curcumin rapidly extinguished McTN in breast CSC, preventing reattachment from suspension. Together, our results support a model in which breast CSCs with cytoskeletal alterations that promote McTN can mediate attachment and metastasis but might be targeted by curcumin as an anti-metastatic strategy.

Corresponding Author: Stuart S. Martin University of Maryland School of Medicine Room 10-29, Bressler Research Building 655 West Baltimore Street, Baltimore, MD 21201. Phone: 410-706-6601 Fax: 410-706-6600 ssmartin@som.umaryland.edu..

S.S. Martin and R.A. Whipple are listed as inventors on a patent issued to the University of Maryland regarding microtentacles. No potential conflicts of interest were disclosed by the other authors.

Keywords

Microtentacles; Circulating Tumor Cells; Breast Cancer Stem Cells; Reattachment; Curcumin; Tubulin

Introduction

Advances in primary breast cancer treatment have led to the development of novel therapeutics; however, metastasis, the main cause of cancer-related deaths, remains poorly understood and largely incurable (1). Traditional models of tumorigenesis suggest that malignancies develop in a series of step-wise genetic mutations culminating in the generation of cancer cells able to disseminate and metastasize (2). However, recent evidence strongly suggests that metastasis may be an early event in tumorigenesis (3, 4). The cancer stem cell (CSC) hypothesis offers new insights into tumorigenesis and metastatic progression that may lead to more effective therapies to reduce metastasis. This hypothesis suggests that tumor development and metastasis are driven by a subpopulation of tumor-initiating cells with the ability to form serially transplantable tumors in immunocompromised mice that recapitulate the characteristics and heterogeneity of the original tumor (5). This subpopulation of cancer cells enriched in tumor-initiating potential can be isolated from the tumor bulk by surface markers or functional assays (6, 7). The stem cell properties of self-renewal, multipotency, and chemotherapeutic resistance provide the driving force for tumorigenesis, and would also provide a selective advantage during metastasis as carcinoma cells survive the hostile environment of the circulation and proliferate in distal tissues (7, 8).

CSC markers are expressed on circulating breast cancer cells obtained from the peripheral bloodstream of breast cancer patients (9, 10). CSCs may have additional traits such as increased motility that prime them for successful metastasis (3), supported by recent *in vivo* and patient studies where metastasizing cells were found to display stem cell markers (3, 8, 11-13). CSCs derived from human breast cancer cell lines were shown to have increased metastatic potential in an experimental metastasis model using NOD/SCID mice (14). Using a PyMT model of mammary tumorigenesis, early metastatic cells disseminated in the lungs displayed stem cell markers (3). Additionally, immunostaining revealed disseminated tumor cells in the bone marrow of breast cancer patients express the breast CSC phenotype (12).

While the CSC theory has been adapted to encompass primary tumor growth in epithelial cancers of many origins, less has been uncovered about its implications for metastasis. Cytoskeletal changes are a critical component of the metastatic cascade, as epithelial cells must undergo cytoskeletal alterations that allow them to intravasate into the bloodstream, withstand the physical pressures of the shear forces in circulation, and extravasate into distant tissues. Cytoskeletal alterations are crucial to the process of metastatic dissemination, as carcinoma cells must alter their morphology to move themselves from the site of origin and migrate throughout the body. Interestingly, studies suggest that circulating CSCs have a more deformable cytoskeleton than more differentiated cells (15), but the specific

cytoskeletal alterations in CSCs compared to normal tissue or the tumor bulk remain unknown.

We have previously identified microtentacles (McTNs), tubulin-based protrusions of the plasma membrane of mouse and human mammary epithelial cells (MECs), as novel cellular structures that form in response to extracellular matrix detachment (16). McTNs are tubulin-based, and mechanistically distinct from actin-based invadopodia and filopodia (16, 17). They promote the reattachment of suspended carcinoma cells, a crucial step in metastasis by which circulating tumor cells (CTCs) exit the bloodstream (16, 18-20). Experimental metastasis studies reveal that promotion of McTNs increases lung retention of CTCs (17, 20). Interestingly, an *in vivo* study using colon carcinoma cells demonstrated that attachment of CTCs to the microvascular endothelium is dependent on tubulin and enhanced by actin depolymerization (21), matching the mechanism underlying McTN formation.

Microtubules may be regulated by multiple post-translational modifications (22, 23). We have previously shown that detyrosinated α-tubulin is enriched in McTNs (16, 18, 24). Detyrosinated tubulin (Glu-tubulin) is formed by the removal of the carboxy-terminal tyrosine on α-tubulin by a tubulin-specific carboxypeptidase (TCP), exposing a glutamic acid residue (25). This reaction is reversed by tubulin tyrosine ligase (TTL). Microtubules composed of Glu-tubulin have a vastly increased stability *in vivo*, persisting for hours rather than the 3 to 5 minutes seen in microtubules composed of Tyr-tubulin (25). Importantly, tubulin detyrosination in breast cancer predicts poor prognosis and metastasis (26, 27). Furthermore, detyrosinated microtubules preferentially associate with the intermediate filament vimentin (28), which can enhance McTN formation (18). The tyrosination status of tubulin in breast CSCs in unknown, but studies in neuroblastoma suggest that detyrosinated tubulin may increase in less differentiated, more stem-like cancer cells (29).

The CSC hypothesis suggests that by identifying the specific subpopulation of cells responsible for tumorigenesis, we may be able to identify or design more highly selective targeted therapeutics. Curcumin, a dietary polyphenol found in the spice turmeric, is generating significant research interest due to its anti-tumor properties. Curcumin has been studied as a chemopreventive agent in a variety of cancers (hematological, breast, gastrointestinal, liver, prostate) and as an inhibitor of metastasis (30). It was recently shown to selectively inhibit the growth and self-renewal of breast tumor stem cells via downregulation of Wnt signaling (31), but also has significant effects on the cytoskeleton.

Given the recent findings that CSCs may play a crucial role in metastasis and CSCs may undergo cytoskeletal alterations, we investigated the relationship between stemness and McTNs. Flow cytometry was used to correlate the stem-like surface marker phenotypes of a panel of breast cancer cell lines with their McTN frequencies and metastatic potential. Flow cytometry of a human MEC line with significant and discrete subpopulations of stem-like and non-stem-like cells was used to investigate differences in McTNs, cytoskeletal alterations, and reattachment efficiency between stem-like and non-stem-like subpopulations from an isogenic background. We specifically examined the protein levels and organization of detyrosinated tubulin and vimentin, since these cytoskeletal components play a role in McTN formation (16, 18). Furthermore, we explored whether the stem-cell targeting agent

curcumin could therapeutically inhibit McTNs on CSCs. Our results identify that CSCs have elevated McTNs which promote more efficient reattachment and reveal novel mechanisms to reduce metastasis by targeting these cytoskeletal alterations.

Materials and Methods

Cell Culture and Chemical Compounds

HMLE cells (32) were generously provided by Dr. Jing Yang (University of California, San Diego) and grown in MEGM complete medium (Lonza) at 37°C in 5% CO_2. SkBr3, MDA-MB-468, BT-549, Hs578T, MDA-MB-231, and MDA-MB-436 cells obtained from the American Type Culture Collection, which authenticates the cell lines by short-tandem repeat DNA testing (Manassas, VA), were used within 6 months of resuscitation and grown in DMEM (Mediatech) supplemented with 10% fetal bovine serum (FBS, Atlanta Biologicals, Lawrenceville, GA) and penicillin-streptomycin (100 μg/mL, Gemini Bioproducts, West Sacramento, CA) at 37°C in 5% CO_2. Colchicine and curcumin were obtained from Sigma (St. Louis, MO). Staurosporine was obtained from EMD Millipore (Darmstadt, Germany).

Flow cytometry analysis and cell sorting

Cells were trypsinized, washed twice with PBS by centrifugation (1000 rpm, 5 minutes), and blocked (0.5% BSA/PBS) for 10 minutes. Cells were then incubated with the antibodies anti-CD44 (Clone G44-26) and anti-CD24 (Clone ML5) from BD Biosciences (San Jose, CA) or isotype controls according to manufacturer's instructions. Cells were sorted using BD FACSAria and analyzed using BD FACSDiva software.

Cell Viability

CellTiter 96 AQ_{ueous} One Solution (Promega) was added according to the manufacturer's recommendations to determine cell viability. Absorbance was measured using a Biotek Synergy HT Multidetection Microplate Reader. All values are shown as mean ± SD of at least triplicate samples.

Western Blotting

Sorted HMLE cells were allowed to readjust to culture conditions for 24 hours before cells were harvested as previously described (18). Western blotting was performed using NuPage gels (Life Technologies). Primary antibodies for CD44 (EPR1013Y, abcam), vimentin (V9, Santa Cruz Biotechnology), detyrosinated tubulin (abcam), α-tubulin (DM1A, Sigma), GAPDH (6C5, Santa Cruz Biotechnology), and poly-(ADP-ribose)-polymerase (PARP) (Cell Signaling) were used at manufacturer's recommended dilutions.

Immunofluorescence

For suspended immunofluorescence, sorted HMLE subpopulations were suspended for 30 minutes in growth media in Ultra-Low Attachment plates (Corning). Cells were then gently centrifuged onto poly-L-lysine coated glass coverslips and fixed in 3.7% formaldehyde/PBS (10 minutes). For attached immunofluorescence, cells were grown on glass coverslips and then fixed in 3.7% formaldehyde/PBS (10 minutes). Cells were permeabilized (0.25% Triton

X-100/PBS, 10 minutes), and blocked for 1 hour (PBS/5% bovine serum albumin (BSA)/ 0.5% NP40). Immunostaining was performed overnight at 4°C (PBS/2.5% BSA/0.5% NP-40) using detyrosinated (Glu) tubulin (abcam) and vimentin (V9, Santa Cruz Biotechnology). Alexa-conjugated anti-IgG antibodies (Molecular Probes) were used for secondary detection and Hoechst 33342 (Sigma) was used for nuclear staining. Images were acquired using an Olympus FV1000 laser scanning confocal microscope (Olympus, Center Valley, PA). Images were taken with identical microscope settings. Z-stacks were imaged as maximum intensity projections using ImageJ (NIH, Bethesda, MD).

Live Cell Imaging and Microtentacle Scoring

Cells were suspended in growth media without Phenol Red over Ultra-Low Attachment plates (Corning) for 30 minutes. Cells were either counted live (18) or fixed (33) as previously described. 100 or more single cells per well were scored blindly for microtentacles by considering cells with two or more microtentacles extending greater than the radius of the cell body as positive, with a minimum of 300 cells counted per condition per trial. All values are shown as mean ± SD of three independent experiments.

Mammosphere Culture and Imaging

HMLE and BT-549 cells were seeded at a concentration of 10,000 cells/mL in Complete Mammocult media (StemCell Technologies, Vancouver, BC, Canada) in Ultra-Low Attachment plates (Corning) and grown according to manufacturer's directions. Mammospheres were infected for 24 hours with a custom GFP-membrane targeted adenovirus (Ad-GFP-mem, Vector Biolabs, Philadelphia, PA), generated from GFP-membrane targeted AcGFP1-Mem plasmid (Clontech, Mountain View, CA). Mammospheres were collected into DMEM without Phenol Red containing CellMask Orange (1:5,000) and incubated for 20 minutes in a glass bottom dish (MatTek Corporation, Ashland, MA) then imaged on an Olympus FV1000 laser scanning confocal microscope. Three-dimensional surface rendering was done using Volocity software (Perkin Elmer, Waltham, MA). For colchicine wash-in experiments, mammospheres were imaged and colchicine (50 μM final concentration) was added for 10 minutes for time-lapse confocal microscopy and images were processed using ImageJ (1 frame/second).

Cell-electrode impedance attachment assay

Real-time monitoring of cellular reattachment from suspension was measured using an electrical impedance assay with an xCELLigence RTCA SP real-time cell sensing device (Roche Applied Science, Indianapolis, IN). HMLE sorted subpopulations (20,000 cells) were seeded into E-plates containing growth medium, vehicle (0.1% DMSO), or colchicine (50 μM final concentration). BT-549 cells were pre-treated for 6 hours with vehicle or 50 μM curcumin, then were added (20,000 cells) to E-plates containing vehicle or drug, respectively. Impedance was measured every 3 minutes for 3 hours. The attachment rate is expressed as the cell index, or the change in electrical impedance at each time point, with values expressed as the cell index ± SD of triplicate wells. Three independent trials were conducted.

Statistical Methods

Significance was determined by Student's *t*-test.

Results

Microtentacles correlate with cancer stem cell (CSC) character in a panel of breast cancer cell lines

We have previously demonstrated that McTNs are more abundant in metastatic breast carcinoma cells lines (18), and given the increasing evidence that CSCs sustain a metastatic advantage (3, 8, 11-13), we investigated whether there was a relationship between breast CSCs and McTNs. Using flow cytometry, the proportion of cells with a stem cell surface marker phenotype ($CD44^{hi}/CD24^{lo}$) and non-stem cell surface marker phenotype ($CD44^{lo}/CD24^{hi}$) were examined across a panel of breast cancer cell lines for which we have already characterized McTNs (18). This analysis demonstrated a positive correlation between the proportion of stem-like subpopulations in a given breast cancer cell line, the relative abundance of McTNs in that cell line, and the cell line's metastatic capabilities (34, 35) (Table 1).

Stem-like mammary epithelial cells have increased microtentacles

To directly test the relationship between stem cell character and McTNs, an immortalized, non-tumorigenic human MEC line, HMLE, was used, which contains distinctive and discrete naturally-present subpopulations of both stem-like and non-stem-like cells (36). We prioritized analysis of the HMLE cell line due to the even distribution and clear separation of stem-like and non-stem-like fractions, which would allow efficient flow sorting of these subpopulations. The isogenic background of the HMLE cell line also provides a more reliable system to ensure that differences in McTN frequency would result from differences in intrinsic stem cell properties and minimize the confounding factors that arise from transformation or genetic variability between different breast cancer cell lines.

Blinded quantitation of McTNs from separated HMLE stem-like and non-stem-like subpopulations (Fig. 1A) was performed while the cells were detached (Fig. 1B). Interestingly, there was over a 2-fold increase in McTN frequencies in the stem-like compared to the non-stem-like subpopulation ($p \leq 0.00005$, $n=3$). The suspended cells from the stem-like population exhibited long, flexible McTNs (arrows), which are absent on the non-stem-like cells (Fig. 1C).

Stem-like mammary epithelial cells have microtentacle-promoting cytoskeletal alterations

Given our previous findings that vimentin and detyrosinated (Glu) tubulin can increase McTNs, we investigated whether these cytoskeletal alterations may contribute to the observed increase in McTNs in the stem-like subpopulation. Western blot analysis revealed an increase in protein levels of vimentin and Glu-tubulin in the stem-like compared to the non-stem-like HMLE subpopulation (Fig. 2A).

After confirming an increase in vimentin expression and Glu-tubulin in the stem-like HMLE subpopulation (Fig. 2A), we used immunofluorescence to distinguish protein localization

and organization between the stem-like and non-stem-like subpopulations. Immunofluorescence of attached HMLE subpopulations demonstrates that protein organization differs, with prominent vimentin networks that colocalize with bundled, filamentous Glu-tubulin in the stem-like subpopulation, while vimentin and Glu-tubulin in the non-stem-like subpopulation are diffuse and non-filamentous (Fig. 2B). Additionally, immunofluorescence performed on suspended subpopulations of HMLEs cells indicates McTNs in the stem-like subpopulation are enriched in Glu-tubulin and vimentin (Fig. 2C, f and g), while the non-stem-like subpopulation lacks both McTNs and a well-defined network of Glu-tubulin and vimentin (Fig. 2C, b and c).

Mammary stem-like cells have increased tubulin-dependent initial reattachment

Because previous studies have indicated that McTNs aid tumor cell reattachment, we sought to determine if the increased McTNs in the stem-cell subpopulation influence attachment (16, 18-20, 24). We compared the ability of the subpopulations to reattach from suspension by real-time electrical impedance. The stem-like cells exhibited significantly faster initial reattachment (Fig. 3A). Phase-contrast imaging shows that stem-like cells began to reattach and spread in as early as 30 minutes (Fig. 3B) and nearly all were attached by 3 hours (Fig. 3B, h), while the non-stem-like cells remained mainly in suspension by 3 hours, with only a few cells beginning to reattach and spread (Fig. 3B, d). Furthermore, reattachment differences between the stem-like and non-stem-like subpopulations are not due to toxicity, as treatment with colchicine produced no difference in viability between the subpopulations over the time period of attachment (Supplemental Fig. 1).

To determine if the differences in initial reattachment were due to the observed differences in McTNs, impedance assays were performed on the sorted subpopulations with vehicle or colchicine (50 μM), a microtubule polymerization inhibitor that rapidly reduces McTNs (16). Colchicine treatment reduced the initial reattachment in both the stem-like and non-stem-like subpopulations (Fig. 3A), indicating that the observed reattachment was tubulin-based, matching the mechanism of McTN formation and CTC adhesion to the capillary endothelium *in vivo* (16, 21). Although the stem-like subpopulation formed significantly more McTNs than the non-stem-like subpopulation (Fig. 1B), the non-stem-like subpopulation still produced tubulin-based McTNs, albeit at a much lower frequency, and thus was also susceptible to a further reduction in attachment efficiency when treated with colchicine (Fig. 3A).

Microtentacles persist in mammospheres

As a novel cellular structure, the functional role of McTNs is still being explored. We have shown that McTNs on suspended breast cancer cells allow them to penetrate between endothelial cells, facilitating the initial steps in reattachment from circulation (24). We have also shown that McTNs promote cellular aggregation, where McTNs encircle adjacent cells (16, 19, 33). Since McTNs promote short-term homotypic aggregation of breast epithelial cells, we sought to determine whether McTNs may play a similar role in the structure of mammospheres arising during long-term growth. Mammosphere formation is an key functional assay for assessing stem cell character, in which growth as non-adherent spheres enriches for mammary stem-like cells (7). HMLE cells were cultivated as mammospheres

over 7 days, membrane-stained with CellMask Orange, and gently pipetted into glass-bottomed dishes for live-cell confocal microscopy. Long, motile, and dynamic protrusions from the cells were observed along the edges of mammospheres (Fig. 4A, a, black arrows and Supplemental Movie 1A), which were abolished upon the addition of colchicine (Fig. 4A, b, and Supplemental Movie 1B), further demonstrating that the observed protrusions are tubulin-based McTNs.

Having established that dynamic McTNs persisted on the surface of cells in mammospheres, we further investigated if McTNs also penetrated through the three-dimensional structure of mammospheres. Both HMLE and tumorigenic BT-549 cells were cultivated as mammospheres, and transduced with GFP targeted to the cell membrane in order to visualize McTNs from individual cells. The entire mammosphere was subsequently stained with CellMask Orange and transferred to a glass-bottom dish for live-cell confocal microscopy. Three-dimensional computer rendering of these mammospheres reveals that cells within mammospheres exhibit long, flexible protrusions which encircle adjacent cells within the mammosphere and penetrate between cell-cell junctions in the mammosphere walls (Fig. 4B, white arrows, and Supplementary Movies 2-5). While encirclement of adjacent cells with McTNs contributes to short-term cell aggregation (33), this evidence indicates that McTNs can persist between adjacent cells during mammosphere development over many days.

Stem-cell targeting agent Curcumin reduces microtentacles and reattachment

Having demonstrated that McTNs are increased in the stem-like subpopulation and persist in mammospheres, we sought to determine if pharmacological targeting of breast cancer stem cells might also inhibit McTNs. We investigated whether curcumin, a dietary polyphenol inhibitor of Wnt signaling shown to inhibit breast cancer stem cells (31) would have an effect on McTN levels and function. Since the BT-549 breast cancer cell line has both a high proportion of stem-cell character and high levels of microtentacles (Table 1) and has previously been shown to be responsive to short term, high dose treatments of curcumin (37), we examined the effect of curcumin on CSC character, McTN formation, and reattachment efficiency in BT-549 cells. Curcumin was previously shown to reduce stem cell signaling as early as 12 hours (31), but can inhibit motility as quickly as 10 minutes when given in high doses (38). Given curcumin's wide-ranging yet rapid effects, we determined if curcumin could affect the CSC subpopulation and McTNs after a relatively short 6 hour treatment. First, we investigated any potential toxicity from curcumin treatment that could potentially confound future studies. A cell viability assay determined that there was no significant loss of cell viability at 6 hours over a dose range of curcumin (Fig. 5A). To further ensure that curcumin treatment was not inducing apoptosis, cells were assayed for poly-(ADP-ribose)-polymerase (PARP) cleavage. Treatment with staurosporine (16h, 1 μM) induced robust PARP cleavage as a positive control, but treatment with a dose range of curcumin (6h) revealed no cleaved PARP (Fig. 5B); these findings indicate that curcumin's effects on CSC characteristics and McTNs are independent of toxicity and apoptosis.

Because curcumin has been shown to be well-tolerated even at very high doses in patients (30), the highest dose shown to be non-toxic (50 μM) was prioritized for functional studies.

Doses of 50 μM curcumin have been shown to be non-toxic in many cell lines including: MCF-7 (breast), LnCAP (prostate), PC-3 (prostate), HepG2 (liver) and A-549 (lung) (38, 39). After a 6 hour treatment, curcumin (50 μM) dramatically reduces the percentage of cells expressing the $CD44^{hi}/CD24^{lo}$ stem cell marker phenotype (Fig. 5C, $p \leq 0.005$, $n=3$). Long-term mammosphere formation was also inhibited by curcumin treatment, further confirming that this dose of curcumin inhibits the breast cancer stem cell subpopulation in our model (50 μM, Supplemental Fig. 2). Having established that 50 μM of curcumin treatment for 6 hours was sufficient to affect breast CSCs, we sought to determine whether McTNs were also affected. When BT-549 cells were treated with either vehicle or curcumin (50μM, 6hr) (Fig. 5D), blinded quantitation revealed a significant reduction in McTN frequencies with curcumin treatment (≥2-fold, $p \leq 0.0005$, $n=3$). To test if this curcumin-induced decrease in McTNs impacted the reattachment of breast tumor cells, we compared the ability of vehicle or curcumin-treated (50 μM, 6 hr) BT-549s to reattach from suspension by real-time electrical impedance. Cells were pretreated with vehicle or curcumin for 6 hours and reattachment was monitored in the presence of vehicle or curcumin, respectively. Treatment with curcumin resulted in a significant reduction in reattachment efficiency compared to vehicle (Fig. 5E).

Discussion

The cytoskeletal dynamics of CTCs are a crucial determinant of their ability to survive the shear forces of the circulatory system and reattach to distal sites for eventual metastatic outgrowth. CSCs may have a more deformable cytoskeleton, giving them a survival advantage in the bloodstream over more differentiated cells (15), but it is uncertain which cytoskeletal components are specifically altered in more stem-like cells. We previously reported that MECs produce novel tubulin-based protrusions of the plasma membrane termed microtentacles (McTNs) upon detachment and suspension (16). In a normal epithelial cell, the outward expansion of microtubules is counteracted by the inward-directed force of the actin cortex, a balance termed the cellular tensegrity model (40). Cytoskeletal dysregulation in tumor cells disrupts tensegrity, allowing for the formation of McTNs in suspended breast cancer cells (19). These McTNs facilitate reattachment, where McTNs penetrate endothelial cell layers and promote retention in the lungs of living mice in experimental metastasis assays (20, 24). Here, we report for the first time that breast cancer cell lines with high proportions of cells expressing the breast CSC surface marker phenotype, $CD44^{hi}/CD24^{lo}$, are associated with an elevated level of McTNs. While this correlation between the breast CSC phenotype and McTNs was established using many cell lines (Table 1), further analysis was prioritized using the isogenic HMLE model system, which has clearly defined CSC and non-CSC subpopulations and the BT-549 cell line, which is highly enriched in the CSC surface marker phenotype, has high levels of McTNs, and has previously been reported to rapidly respond to curcumin treatment (37).

Using the HMLE cell line as an isogenic model of naturally arising stem-like and non-stem-like subpopulations, we further demonstrate that the stem-like subpopulation of MECs have significantly increased levels of McTNs and enhanced reattachment. This data suggests that not only are breast CSCs more efficient at tumor formation, they are primed for more

successful metastasis by promoting McTN formation, which facilitates attachment at distal sites.

Microtentacles may be stabilized through a variety of mechanisms, including α-tubulin detyrosination and upregulation of the intermediate filament vimentin (reviewed in (19)). Protein analysis and immunofluorescence of attached and suspended HMLE stem-like and non-stem-like cells suggest that breast CSCs promote McTN formation through tubulin detyrosination and vimentin upregulation. Both Glu-tubulin and vimentin enhance McTN formation and signify poor patient prognosis (26, 27, 41), but until this study had not been identified as concordant cytoskeletal alterations specific to the breast CSC subpopulation. Furthermore, our findings suggest that increased tubulin detyrosination and vimentin expression provide a selective advantage to breast CSCs during the metastatic process, as they enhance McTN formation and can promote reattachment. Our novel finding that stem-like breast cells have a dramatically faster reattachment rate provides compelling evidence that breast CSCs are inherently more capable of metastatic dissemination. Tubulin has long been a popular target for cancer therapeutics given its role in cell division, yet widespread toxicity and acquired drug resistance limits the utility of tubulin-targeted agents (42). Our data demonstrates for the first time that the stem-like subpopulation of breast cells are enriched in detyrosinated (Glu) tubulin and vimentin, cytoskeletal modifications that support the increased McTN frequency observed in the breast stem-like subpopulations. This novel finding that breast stem cells have elevated, stable microtubules that enhance McTN formation suggests that the development of therapies aimed at this specific subset of Glu-microtubules may be more efficacious in reducing metastasis and generally less toxic than therapies affecting microtubules indiscriminately.

The growth of single cells under non-adherent conditions into spheres termed mammospheres has become an important assay for breast stem cell character, as mammosphere growth depends on the presence of self-renewing stem cells (7). In this study, we show that dynamic, tubulin-dependent McTNs persist on the outer surface of mammospheres after 7 days of growth under non-adherent conditions. Our confocal imaging data suggests that McTNs on these breast CSCs penetrate between cell-cell junctions, encircling adjacent cells within the mammosphere wall, extending the role of McTNs beyond facilitation of short-term homotypic aggregation. Our previous studies focused on the generation of McTNs on single, suspended cells; here, we show that cells growing attached to one another in a mammosphere are still able to form McTNs on areas of the cell membrane exposed to the environment. Given our novel findings that McTN persist during long-term mammosphere growth and remain reactive to the environment of suspension, it is possible that McTNs on circulating CSCs may also aid in the formation and even reattachment of clusters of CTCs. Characterization of CTCs is an emerging field, where the identification and biological significance of CTC clusters in the bloodstream is poorly understood. *Ex vivo* and *in vivo* experiments using single cell suspensions of metastatic breast carcinoma cells reveal the formation of homotypic aggregates at the site of attachment to the endothelial wall (43), and a recently-developed enrichment-free immunofluorescence detection method has identified circulating aggregates of tumor cells in bloodstream of patients with various epithelial cancers (44). Regardless of whether the aggregates are

formed during transit in the bloodstream or following the adhesion of an initial single cell, McTNs could be facilitating this cluster reattachment of breast carcinoma cells to the vascular endothelium. Similar to the McTNs we report here both within the mammosphere wall and on the outer surface of the mammosphere, McTNs on circulating CTC clusters could both aid in the aggregation of CTC clusters and in their attachment to the endothelium.

Recently, Shibue *et al* have identified a novel cellular structure, termed filopodia-like protrusions (FLPs), with similarities to McTNs (45, 46). FLPs are actin-based protrusions produced by attached breast cancer cells which interact with the ECM via integrin β_1 to aid in establishing primary tumors and metastatic lesions. Importantly, when using the same HMLE model for stem-like and non-stem-like as the present study, FLPs were more numerous and longer lived in the stem-like subpopulation. Collectively, this data suggests that breast cancer stem cells have unique cytoskeletal modifications that promote metastatic spread. Like McTNs, FLPs are increased in more metastatic cell lines. In contrast, McTNs are tubulin-based protrusions generated on suspended cells while FLPs are actin-based structures arising on ECM-attached cells. Further distinguishing McTNs and FLPs, activation of actin-severing protein cofilin enhances McTN formation while impairing FLP formation (33, 46). These differences in cytoskeletal structure underscore the need for careful consideration of cytoskeletal-targeted chemotherapeutics, as the initial stages of CTC reattachment depend on tubulin while transendothelial migration and colonization rely on actin (17, 21).

While there are many questions remaining about stem cell biology and CSCs, the identification of surface markers that enrich for tumor-initiating cells has effectively demonstrated that in many epithelial cancers, only a subset of cells are capable of efficient tumorigenesis and metastasis. The next step towards clinical utility of the cancer stem cell theory is to identify specific therapeutic targets to inhibit CSCs while sparing normal epithelial cells. Our data reveal that a short term treatment with high doses of curcumin is sufficient to reduce the CSC surface marker phenotype without affecting viability. For the first time, we demonstrate that short-term, high-dose curcumin treatment can inhibit McTN formation and prevent reattachment from suspension. These data demonstrate that stem-cell targeted therapies can have rapid effects on the surface markers and cytoskeletal organization of CSCs that are independent of effects on growth and do not require long-term selection of different subpopulations. Since curcumin is well-tolerated even at very high doses in patients (30), and non-toxic in many cell lines (38, 39), it is also possible that the side effects of curcumin treatment may be relatively low. Our finding that curcumin inhibits McTNs and reattachment may provide a mechanism for previous studies in which curcumin treatment was shown to significantly reduce breast cancer cell adhesion in a parallel plate flow chamber assay (47), where a loss of McTNs could prevent the breast cancer cells from making the initial attachments required for adhesion. Additionally, data showing that treatment with curcumin inhibits spontaneous metastasis of human breast cancer to the lung in a mouse xenograft model supports our model where inhibition of McTNs prevents cancer cell retention in the lungs, serving as a potential strategy to reduce metastasis (48).

Curcumin has been shown to have pleiotropic mechanisms of action (reviewed in (30)), exerting effects by directly interacting with targets (at least 33 different proteins) or by modulating gene expression through multiple transcriptional factors, such as NFκB and Wnt/β-catenin (30). We and others have shown that curcumin inhibits the breast CSC subpopulation (31); however, in the present study we report that McTNs are a novel target for curcumin and can inhibit CSC reattachment. While the specific mechanism of action in McTN reduction is under current investigation, it remains possible that curcumin is reducing McTNs and inhibiting reattachment through numerous mechanisms, beyond its direct effects on the cytoskeleton. Fluorescence spectroscopy and FRET indicate that curcumin may bind directly to tubulin, the major component of McTNs (49, 50). Several studies in breast and prostate cancer cell lines suggest that curcumin can interfere with microtubule dynamics and F-actin architecture in a dose, time, and cell-line dependent manner (38, 49, 51, 52). Curcumin's specific effects on cytoskeleton of breast CSCs compared to other more well-differentiated normal and malignant epithelial cells and its disruption of McTN formation are the subject of ongoing investigation in our laboratory.

While the current study focuses on the cytoskeletal dynamics of cultured human breast tumor cells subjected to free-floating conditions, these conditions cannot completely recreate the complexity of human disease. Previous studies in animal models from our lab and others have shown that CTCs reattach to blood vessel walls with an actin-independent, tubulin-dependent cytoskeletal mechanism (20, 21) that matches the McTNs we have identified within the stem-like subpopulation of cultured breast tumor cells. New methods for imaging McTN-based reattachment of CTCs within intact blood vessels are under development in our laboratory. To extend these findings into breast cancer patients will require new technology to rapidly isolate live and intact CTCs for dynamic cytoskeletal studies. Such rapid CTC isolation technology is under intense development by many groups and will be used when it is available to determine if circulating breast CSCs from human patients produce McTNs that aid in their reattachment at distal sites.

The data presented here support a model in which breast CSCs are not only highly tumorigenic, but are primed for more successful metastasis due to cytoskeletal alterations leading to increased production of dynamic McTNs, which promote reattachment. Curcumin's ability to reduce McTNs and inhibit reattachment makes curcumin an intriguing potential chemotherapeutic that could not only inhibit the outgrowth of metastases, but also reduce the potential for circulating CSCs to reattach and establish deadly metastases.

Supplementary Material

Refer to Web version on PubMed Central for supplementary material.

Acknowledgments

We would like to thank Dr. Jing Yang of the University of California, San Diego, for kindly providing the HMLE cell line and expertise, and Karen Underwood and Ferenc Livak at the University of Maryland Greenebaum Cancer Center Flow Cytometry Shared Services for flow cytometry sorting and analysis.

Grant Support:

This work was supported by the National Cancer Institute (R01-CA154624), Susan G. Komen Foundation (KG100240) and an Era of Hope Scholar award from the Department of Defense (BC100675).

Abbreviations

CSC	cancer stem cell
CTC	circulating tumor cell
Glu-tubulin	detyrosinated tubulin
McTN	microtentacle
TCP	tubulin carboxypeptidase
TTL	tubulin tyrosine ligase
Vim	vimentin
Stauro	Staurosporine
PARP	poly (ADP-ribose) polymerase
MEC	mammary epithelial cell
FLP	filopodia-like protrusion

References

1. Lu J, Steeg PS, Price JE, Krishnamurthy S, Mani SA, Reuben J, et al. Breast cancer metastasis: challenges and opportunities. Cancer Res. 2009; 69:4951–3. [PubMed: 19470768]
2. Klein CA. Parallel progression of primary tumours and metastases. Nat Rev Cancer. 2009; 9:302–12. [PubMed: 19308069]
3. Weng D, Penzner JH, Song B, Koido S, Calderwood SK, Gong J. Metastasis is an early event in mouse mammary carcinomas and is associated with cells bearing stem cell markers. Breast Cancer Res. 2012; 14:R18. [PubMed: 22277639]
4. Husemann Y, Geigl JB, Schubert F, Musiani P, Meyer M, Burghart E, et al. Systemic spread is an early step in breast cancer. Cancer Cell. 2008; 13:58–68. [PubMed: 18167340]
5. Gupta PB, Chaffer CL, Weinberg RA. Cancer stem cells: mirage or reality? Nat Med. 2009; 15:1010–2. [PubMed: 19734877]
6. Al-Hajj M, Wicha MS, Benito-Hernandez A, Morrison SJ, Clarke MF. Prospective identification of tumorigenic breast cancer cells. Proc Natl Acad Sci U S A. 2003; 100:3983–8. [PubMed: 12629218]
7. Dontu G, Abdallah WM, Foley JM, Jackson KW, Clarke MF, Kawamura MJ, et al. In vitro propagation and transcriptional profiling of human mammary stem/progenitor cells. Genes Dev. 2003; 17:1253–70. [PubMed: 12756227]
8. Lawson JC, Blatch GL, Edkins AL. Cancer stem cells in breast cancer and metastasis. Breast Cancer Res Treat. 2009; 118:241–54. [PubMed: 19731012]
9. Wang N, Shi L, Li H, Hu Y, Du W, Liu W, et al. Detection of circulating tumor cells and tumor stem cells in patients with breast cancer by using flow cytometry : A valuable tool for diagnosis and prognosis evaluation. Tumour Biol. 2012; 33:561–9. [PubMed: 22241087]
10. Aktas B, Tewes M, Fehm T, Hauch S, Kimmig R, Kasimir-Bauer S. Stem cell and epithelial-mesenchymal transition markers are frequently overexpressed in circulating tumor cells of metastatic breast cancer patients. Breast Cancer Res. 2009; 11:R46. [PubMed: 19589136]
11. Abraham BK, Fritz P, McClellan M, Hauptvogel P, Athelogou M, Brauch H. Prevalence of CD44+/CD24−/low cells in breast cancer may not be associated with clinical outcome but may favor distant metastasis. Clin Cancer Res. 2005; 11:1154–9. [PubMed: 15709183]

12. Balic M, Lin H, Young L, Hawes D, Giuliano A, McNamara G, et al. Most early disseminated cancer cells detected in bone marrow of breast cancer patients have a putative breast cancer stem cell phenotype. Clin Cancer Res. 2006; 12:5615–21. [PubMed: 17020963]
13. Liu H, Patel MR, Prescher JA, Patsialou A, Qian D, Lin J, et al. Cancer stem cells from human breast tumors are involved in spontaneous metastases in orthotopic mouse models. Proc Natl Acad Sci U S A. 2010; 107:18115–20. [PubMed: 20921380]
14. Charafe-Jauffret E, Ginestier C, Iovino F, Wicinski J, Cervera N, Finetti P, et al. Breast cancer cell lines contain functional cancer stem cells with metastatic capacity and a distinct molecular signature. Cancer Res. 2009; 69:1302–13. [PubMed: 19190339]
15. Zhang W, Kai K, Choi DS, Iwamoto T, Nguyen YH, Wong H, et al. Microfluidics separation reveals the stem-cell-like deformability of tumor-initiating cells. Proc Natl Acad Sci U S A. 2012; 109:18707–12. [PubMed: 23112172]
16. Whipple RA, Cheung AM, Martin SS. Detyrosinated microtubule protrusions in suspended mammary epithelial cells promote reattachment. Exp Cell Res. 2007; 313:1326–36. [PubMed: 17359970]
17. Balzer EM, Whipple RA, Thompson K, Boggs AE, Slovic J, Cho EH, et al. c-Src differentially regulates the functions of microtentacles and invadopodia. Oncogene. 2010; 29:6402–8. [PubMed: 20956943]
18. Whipple RA, Balzer EM, Cho EH, Matrone MA, Yoon JR, Martin SS. Vimentin filaments support extension of tubulin-based microtentacles in detached breast tumor cells. Cancer Res. 2008; 68:5678–88. [PubMed: 18632620]
19. Matrone MA, Whipple RA, Balzer EM, Martin SS. Microtentacles tip the balance of cytoskeletal forces in circulating tumor cells. Cancer Res. 2010; 70:7737–41. [PubMed: 20924109]
20. Matrone MA, Whipple RA, Thompson K, Cho EH, Vitolo MI, Balzer EM, et al. Metastatic breast tumors express increased tau, which promotes microtentacle formation and the reattachment of detached breast tumor cells. Oncogene. 2010; 29:3217–27. [PubMed: 20228842]
21. Korb T, Schluter K, Enns A, Spiegel HU, Senninger N, Nicolson GL, et al. Integrity of actin fibers and microtubules influences metastatic tumor cell adhesion. Exp Cell Res. 2004; 299:236–47. [PubMed: 15302590]
22. Janke C, Bulinski JC. Post-translational regulation of the microtubule cytoskeleton: mechanisms and functions. Nat Rev Mol Cell Biol. 2011; 12:773–86. [PubMed: 22086369]
23. Westermann S, Weber K. Post-translational modifications regulate microtubule function. Nat Rev Mol Cell Biol. 2003; 4:938–47. [PubMed: 14685172]
24. Whipple RA, Matrone MA, Cho EH, Balzer EM, Vitolo MI, Yoon JR, et al. Epithelial-to-mesenchymal transition promotes tubulin detyrosination and microtentacles that enhance endothelial engagement. Cancer Res. 2010; 70:8127–37. [PubMed: 20924103]
25. Kreitzer G, Liao G, Gundersen GG. Detyrosination of tubulin regulates the interaction of intermediate filaments with microtubules in vivo via a kinesin-dependent mechanism. Mol Biol Cell. 1999; 10:1105–18. [PubMed: 10198060]
26. Mialhe A, Lafanechere L, Treilleux I, Peloux N, Dumontet C, Bremond A, et al. Tubulin detyrosination is a frequent occurrence in breast cancers of poor prognosis. Cancer Res. 2001; 61:5024–7. [PubMed: 11431336]
27. Kuroda H, Saito K, Kuroda M, Suzuki Y. Differential expression of glu-tubulin in relation to mammary gland disease. Virchows Arch. 2010; 457:477–82. [PubMed: 20697907]
28. Gurland G, Gundersen GG. Stable, detyrosinated microtubules function to localize vimentin intermediate filaments in fibroblasts. The Journal of cell biology. 1995; 131:1275–90. [PubMed: 8522589]
29. Kato C, Miyazaki K, Nakagawa A, Ohira M, Nakamura Y, Ozaki T, et al. Low expression of human tubulin tyrosine ligase and suppressed tubulin tyrosination/detyrosination cycle are associated with impaired neuronal differentiation in neuroblastomas with poor prognosis. Int J Cancer. 2004; 112:365–75. [PubMed: 15382060]
30. Kunnumakkara AB, Anand P, Aggarwal BB. Curcumin inhibits proliferation, invasion, angiogenesis and metastasis of different cancers through interaction with multiple cell signaling proteins. Cancer letters. 2008; 269:199–225. [PubMed: 18479807]

31. Kakarala M, Brenner DE, Korkaya H, Cheng C, Tazi K, Ginestier C, et al. Targeting breast stem cells with the cancer preventive compounds curcumin and piperine. Breast Cancer Res Treat. 2010; 122:777–85. [PubMed: 19898931]
32. Elenbaas B, Spirio L, Koerner F, Fleming MD, Zimonjic DB, Donaher JL, et al. Human breast cancer cells generated by oncogenic transformation of primary mammary epithelial cells. Genes Dev. 2001; 15:50–65. [PubMed: 11156605]
33. Vitolo MI, Boggs AE, Whipple RA, Yoon JR, Thompson K, Matrone MA, et al. Loss of PTEN induces microtentacles through PI3K-independent activation of cofilin. Oncogene. 2012
34. Sommers CL, Byers SW, Thompson EW, Torri JA, Gelmann EP. Differentiation state and invasiveness of human breast cancer cell lines. Breast Cancer Res Treat. 1994; 31:325–35. [PubMed: 7881109]
35. Blick T, Widodo E, Hugo H, Waltham M, Lenburg ME, Neve RM, et al. Epithelial mesenchymal transition traits in human breast cancer cell lines. Clin Exp Metastasis. 2008; 25:629–42. [PubMed: 18461285]
36. Mani SA, Guo W, Liao MJ, Eaton EN, Ayyanan A, Zhou AY, et al. The epithelial-mesenchymal transition generates cells with properties of stem cells. Cell. 2008; 133:704–15. [PubMed: 18485877]
37. Mukhopadhyay A, Banerjee S, Stafford LJ, Xia C, Liu M, Aggarwal BB. Curcumin-induced suppression of cell proliferation correlates with down-regulation of cyclin D1 expression and CDK4-mediated retinoblastoma protein phosphorylation. Oncogene. 2002; 21:8852–61. [PubMed: 12483537]
38. Holy J. Curcumin inhibits cell motility and alters microfilament organization and function in prostate cancer cells. Cell motility and the cytoskeleton. 2004; 58:253–68. [PubMed: 15236356]
39. Arnal N, Tacconi de Alaniz MJ, Marra CA. Natural polyphenols may ameliorate damage induced by copper overload. Food and chemical toxicology : an international journal published for the British Industrial Biological Research Association. 2012; 50:415–22. [PubMed: 22036966]
40. Ingber DE. Tensegrity I. Cell structure and hierarchical systems biology. J Cell Sci. 2003; 116:1157–73. [PubMed: 12615960]
41. Vora HH, Patel NA, Rajvik KN, Mehta SV, Brahmbhatt BV, Shah MJ, et al. Cytokeratin and vimentin expression in breast cancer. The International journal of biological markers. 2009; 24:38–46. [PubMed: 19404921]
42. Risinger AL, Giles FJ, Mooberry SL. Microtubule dynamics as a target in oncology. Cancer treatment reviews. 2009; 35:255–61. [PubMed: 19117686]
43. Glinsky VV, Glinsky GV, Glinskii OV, Huxley VH, Turk JR, Mossine VV, et al. Intravascular metastatic cancer cell homotypic aggregation at the sites of primary attachment to the endothelium. Cancer Res. 2003; 63:3805–11. [PubMed: 12839977]
44. Cho EH, Wendel M, Luttgen M, Yoshioka C, Marrinucci D, Lazar D, et al. Characterization of circulating tumor cell aggregates identified in patients with epithelial tumors. Physical biology. 2012; 9:016001. [PubMed: 22306705]
45. Shibue T, Brooks MW, Inan MF, Reinhardt F, Weinberg RA. The outgrowth of micrometastases is enabled by the formation of filopodium-like protrusions. Cancer discovery. 2012; 2:706–21. [PubMed: 22609699]
46. Shibue T, Brooks MW, Weinberg RA. An Integrin-Linked Machinery of Cytoskeletal Regulation that Enables Experimental Tumor Initiation and Metastatic Colonization. Cancer Cell. 2013; 24:481–98. [PubMed: 24035453]
47. Palange AL, Di Mascolo D, Singh J, De Franceschi MS, Carallo C, Gnasso A, et al. Modulating the vascular behavior of metastatic breast cancer cells by curcumin treatment. Frontiers in oncology. 2012; 2:161. [PubMed: 23162792]
48. Aggarwal BB, Shishodia S, Takada Y, Banerjee S, Newman RA, Bueso-Ramos CE, et al. Curcumin suppresses the paclitaxel-induced nuclear factor-kappaB pathway in breast cancer cells and inhibits lung metastasis of human breast cancer in nude mice. Clin Cancer Res. 2005; 11:7490–8. [PubMed: 16243823]

49. Gupta KK, Bharne SS, Rathinasamy K, Naik NR, Panda D. Dietary antioxidant curcumin inhibits microtubule assembly through tubulin binding. The FEBS journal. 2006; 273:5320–32. [PubMed: 17069615]

50. Chakraborti S, Das L, Kapoor N, Das A, Dwivedi V, Poddar A, et al. Curcumin recognizes a unique binding site of tubulin. Journal of medicinal chemistry. 2011; 54:6183–96. [PubMed: 21830815]

51. Saab MB, Bec N, Martin M, Estephan E, Cuisinier F, Larroque C, et al. Differential Effect of Curcumin on the Nanomechanics of Normal and Cancerous Mammalian Epithelial Cells. Cell biochemistry and biophysics. 2012

52. Banerjee M, Singh P, Panda D. Curcumin suppresses the dynamic instability of microtubules, activates the mitotic checkpoint and induces apoptosis in MCF-7 cells. The FEBS journal. 2010; 277:3437–48. [PubMed: 20646066]

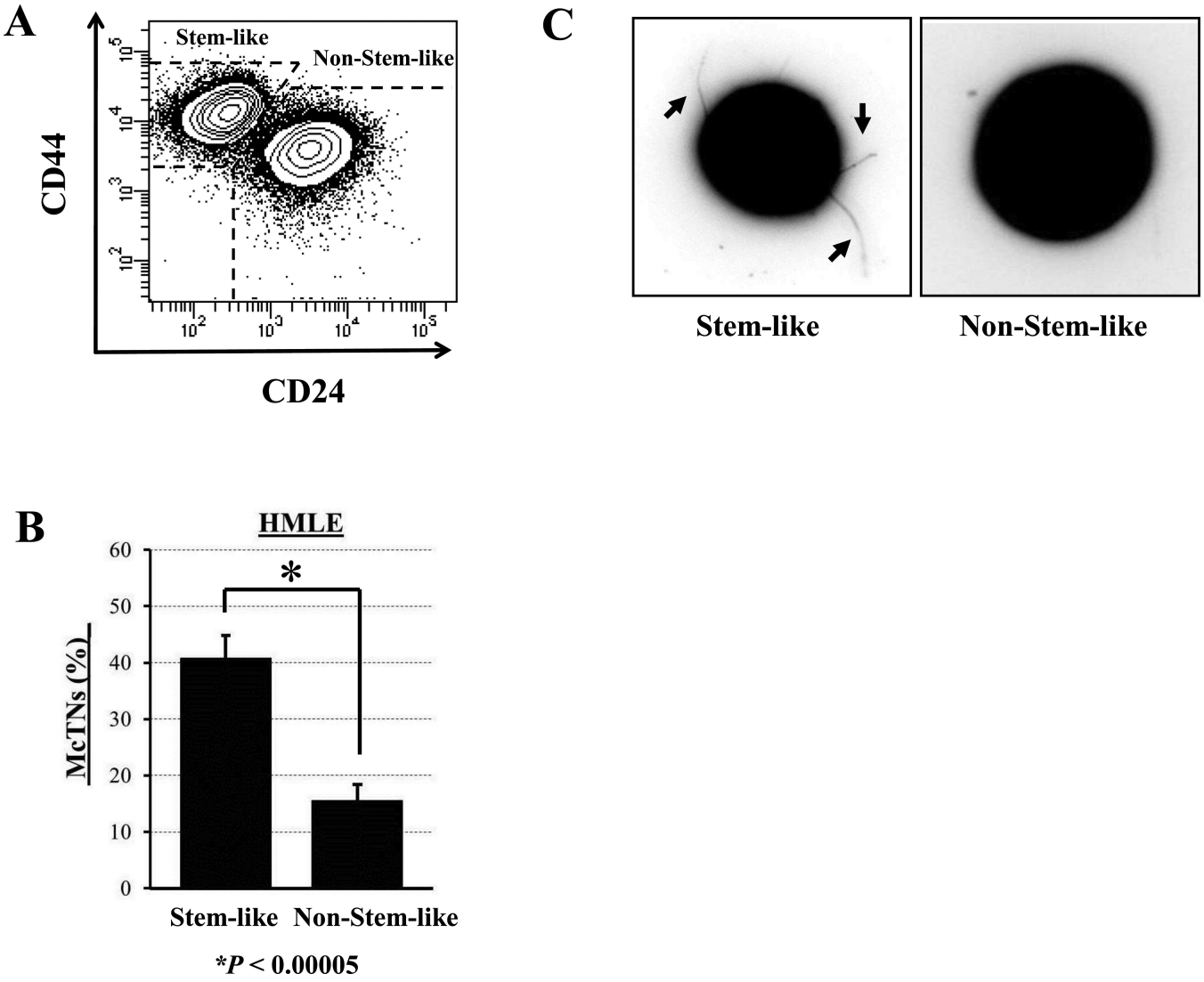

Figure 1. Stem-like mammary epithelial cells have increased microtentacles

A) HMLE cells have distinct subpopulations of stem-like ($CD44^{hi}/CD24^{lo}$) and non-stem-like ($CD44^{lo}/CD24^{hi}$) cells. *B*) Flow sorted stem-like subpopulations of HMLEs display significantly higher microtentacle frequencies than non-stem-like subpopulations. Columns, mean for three blinded experiments where at least 100 CellMask-stained cells were counted, representative of three independent experiments; bars, SD ($P \leq 0.00005$, *t* test, black asterisk). *C*) Phase-contrast images of detached HMLE subpopulations where stem-like HMLEs display increased microtentacles (black arrows) compared to non-stem-like HMLEs.

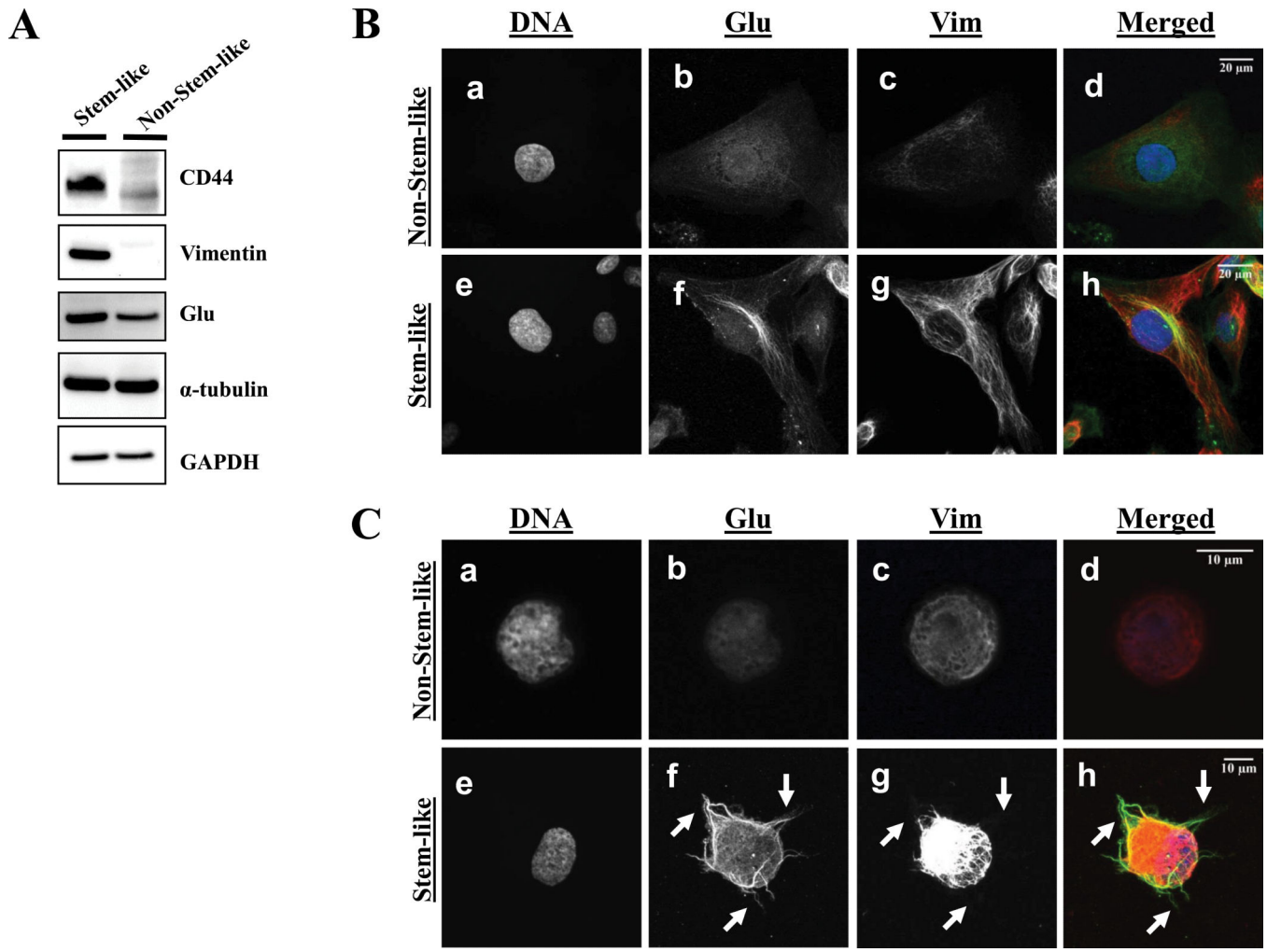

Figure 2. Stem-like mammary epithelial cells have microtentacle-promoting cytoskeletal alterations

A) Representative western blot analysis of HMLE subpopulations shows that stem-like HMLEs have increased vimentin and detyrosinated tubulin (Glu) whereas total α-tubulin and GAPDH are unchanged (cropped). *B*) Attached non-stem-like HMLE cells show weak, diffuse staining for Glu-tubulin (b) and a loss of vimentin protein and organization (c), whereas stem-like HMLE cells display bundling of filamentous Glu-tubulin (f) and a robust network of vimentin filaments (g). Hoechst was used to visualize the nuclei (d, h). *C*) Suspended immunofluorescence where detached HMLE subpopulations were spun down onto glass coverslips and fixed. Immunostaining reveals the presence of Glu-tubulin (f) and vimentin (g) in McTN protrusions (white arrows) in the stem-like HMLE subpopulation but not in the non-stem-like subpopulation (b,c). Hoescht was used to visualize the nuclei (a,e).

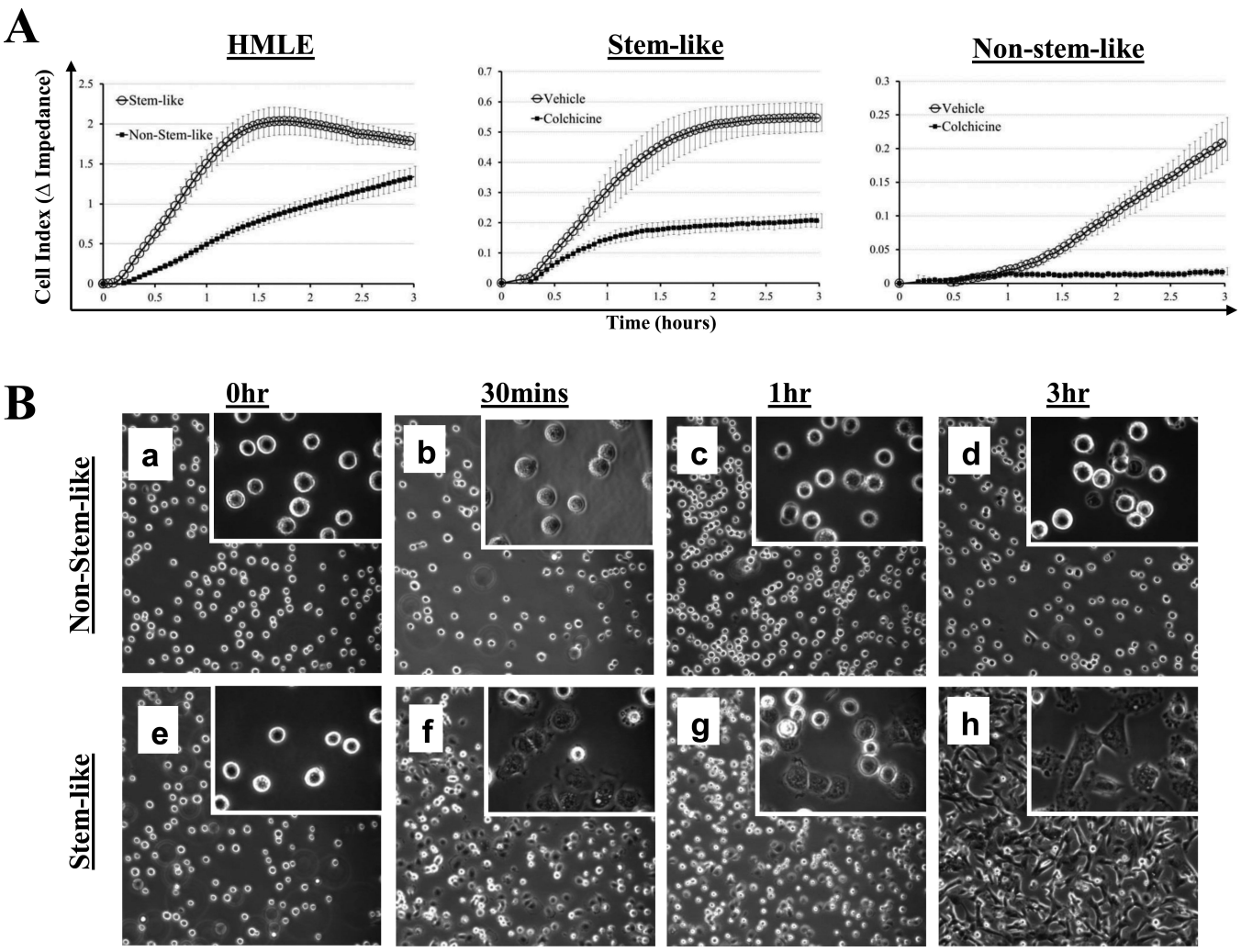

Figure 3. Mammary stem-like cells have increased tubulin-dependent initial reattachment from suspension

A) Stem-like HMLE cells attach at significantly faster rates than non-stem-like HMLE cells as determined by electrical impedance expressed as Cell Index. Stem-like HMLE cells and non-stem-like HMLE cells both have significantly reduced attachment when treated with the microtubule polymerization inhibitor colchicine (50μM). For all reattachment assays: lines=mean for quadruplicate wells; bars=SD; representative graph from three independent experiments is shown. *B*) Phase contrast images of HMLE stem-like (a-d) and non-stem-like (e-h) subpopulations reattaching from suspension. Panels, 10x magnification; Insets, 60x magnification.

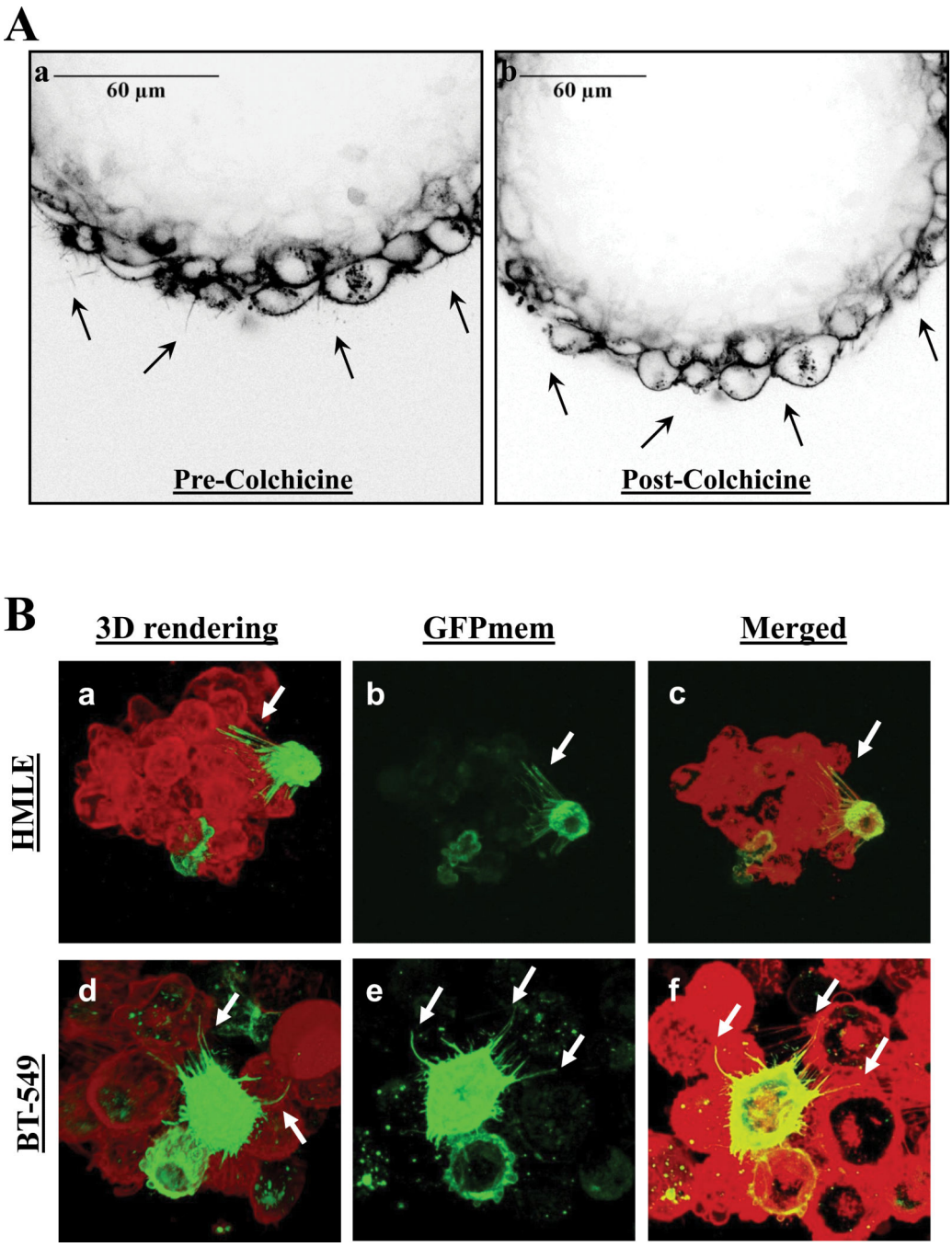

Figure 4. Microtentacles persist in mammospheres

A) Live cell confocal imaging of a HMLE mammosphere stained with CellMask Orange revealing dynamic microtentacles (a, black arrows) that disappear upon treatment with microtubule polymerization inhibitor Colchicine (b, 50μM, 10 minutes). *B*) Live cell confocal imaging of mammospheres stained with CellMask Orange (red) and transduced with GFP-membrane (green) suspended over a glass surface reveals McTNs from the GFP-membrane cell encircling other cells in the mammosphere. Three-dimensional computer-rendered image of HMLE (a) and BT-549 (d) mammospheres viewed from the bottom of the

spheres. GFP-membrane transduced cells reveal long, flexible protrusions (b, e) that encircle other cells in the mammospheres (c, f).

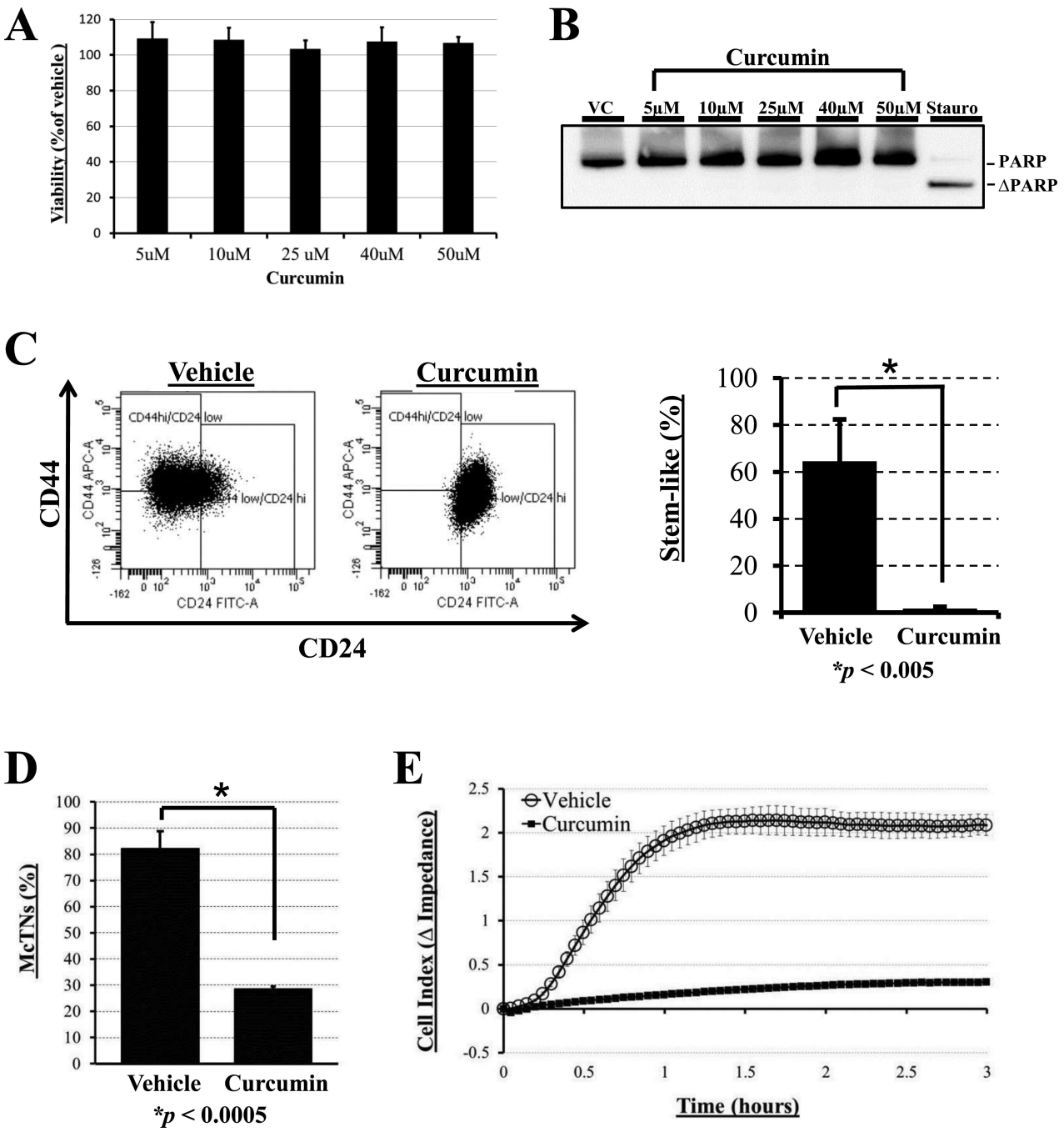

Figure 5. Stem-cell targeting agent Curcumin reduces microtentacles and reattachment

A) Cellular viability assay using CellTiter 96 AQ_{ueous} One Solution (Promega) reveals no significant differences in viability between BT-549 cells treated with doses of curcumin (5, 10, 25, 40, and 50μM) compared to vehicle (DMSO) for 6 hours ($P \geq 0.05$ for each time point). *B*) Western blot analysis reveals no significant cleavage of poly ADP-ribose polymerase (ΔPARP) with up to 50 μM Curcumin exposure for 6 hrs BT-549s, while treatment with 1 μM staurosporine for 16 hrs positively induced PARP cleavage (far right lane). *C*) Treatment with 50 μM Curcumin for 6hr significantly reduces the proportion of

cells in stem-like population as assessed by surface marker phenotype. Columns=mean for three independent experiments where at least 10,000 BT-549 cells per treatment group were analyzed; bars=SD ($P \leq 0.005$, *t* test, black asterisk). *D)* Vehicle-treated BT-549s display significantly higher microtentacle frequencies than BT-549s treated with 50μM curcumin for 6 hours. Columns=mean for three blinded experiments where at least 100 CellMask-stained cells were counted, representative of three independent experiments; bars=SD ($P \leq 0.0005$, *t* test, black asterisk). *E*) Vehicle-treated BT-549s attach at significantly faster rates than BT-549s pretreated with 50μM curcumin for 6 hours and then seeded into E-plates containing vehicle or drug, respectively, as determined by electrical impedance expressed as Cell Index. Lines=mean for quadruplicate wells; bars=SD; representative graph from three independent experiments is shown.

Table 1

Microtentacles correlate with stem-cell surface markers in human breast cancer cell lines

A panel of breast cancer cell lines with an established increasing range of invasiveness, metastatic potential and microtentacle levels were measured by flow cytometry using breast cancer stem cell surface markers CD44 and CD24 for subpopulations of stem-like ($CD44^{hi}/CD24^{lo}$) and non-stem-like cells ($CD44^{lo}/CD24^{hi}$).

Cell Line	SkBr3	MDA-MB-468	Bt549	Hs578t	MDA-MB-231	MDA-MB-436
$CD44^{hi}/CD24^{lo}$ (Stem-like)	0.1% ±0	1.4% ±0.1	76.8% ±0.2	95.1% ±0.2	99.8% ±0	97.4% ±0
$CD44^{lo}/CD24^{hi}$ (Non-stem like)	99.7% ±0	13.1% ±0.6	18.7% ±0.3	5.3% ±0.3	0.1% ±0	0.1% ±0